THE SEESAW MECHANISM AND RENORMALIZATION GROUP EFFECTS

M. LINDNER

Physik Department, Technische Universität München
James-Franck-Str., D-85748 Garching/München, Germany
E-mail: lindner@ph.tum.de

Neutrino mass models predict masses and mixings typically at very high scales, while the measured values are determined at low energies. The renormalization group running which connects models with measurements is discussed in this paper. Analytic formulae for the running which include both Dirac- and Majorana CP phases are provided and they allow a systematic understanding of all effects. Some applications and numerical examples are shown.

1. Introduction

The determination of neutrino masses and mixings has made enormous progress in recent years. Furthermore it is expected that precision neutrino physics will become possible in the future such that the lepton sector may ultimately provide the most precise information on flavour structures. Already now exists enough information to try to understand the patterns of masses and mixings in different models of flavour, but this will become much more interesting in the future with growing precision. One class of models is, for example, given by discrete flavour symmetries which might emerge as unbroken subgroups of broken flavour gauge symmetries. There are different reasons why the scale where an understanding of flavour becomes possible is very high. This has the consequence, that like in the quark sector [1,2] renormalization group (RGE) effects must potentially be taken into account when high energy predictions are compared with low energy measurements. We will show that such RGE effects can be important and that the pattern which needs to be explained at high energies may differ substantially from that at low energies.

2. Running below the seesaw scale

We will discuss neutrino masses which can be described by the lowest-dimensional neutrino mass operator compatible with the gauge symmetries of the Standard Model (SM). This dimension 5 operator reads in the SM

$$\mathscr{L}_\kappa = \frac{1}{4}\kappa_{gf}\,\overline{\ell^{\rm C}_{{\rm L}\,c}}^{g}\varepsilon^{cd}\phi_d\;\ell^f_{{\rm L}b}\varepsilon^{ba}\phi_a + \text{h.c.}\,, \tag{1}$$

and in its minimal supersymmetric extension, the MSSM,

$$\mathscr{L}_\kappa^{\rm MSSM} \;=\; \mathscr{W}_\kappa\big|_{\theta\theta} + \text{h.c.} = -\tfrac{1}{4}\kappa_{gf}\,\mathbb{l}^g_c\varepsilon^{cd}\mathbb{h}^{(2)}_d\;\mathbb{l}^f_b\varepsilon^{ba}\mathbb{h}^{(2)}_a\big|_{\theta\theta} + \text{h.c.}\,. \tag{2}$$

κ_{gf} has mass dimension -1 and is symmetric under interchange of the generation indices f and g, ε is the totally antisymmetric tensor in 2 dimensions, and $\ell^{\rm C}_{\rm L}$ is the charge conjugate of a lepton doublet. $a, b, c, d \in \{1, 2\}$ are $\mathrm{SU}(2)_{\rm L}$ indices. $\mathbb{l}$ and $\mathbb{h}$ denote lepton doublets and the up-type Higgs superfield in the MSSM. After electroweak (EW) symmetry breaking, a Majorana neutrino mass matrix proportional to κ emerges as shown in Fig. 1. The d=5 mass operator describes neutrino masses in a rather model-

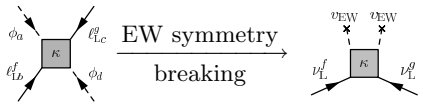

Figure 1. The Majorana mass matrix for light neutrinos from the dimension 5 operator.

independent way to (see e.g. [3]). Integrating out heavy singlet fermions and/or Higgs triplets as for instance in left-right-symmetric extensions of the SM or MSSM leads to tree-level realizations which are usually referred to as type I and type II see-saw mechanisms. The energy dependence of the effective neutrino mass matrix below the scale M_1 where the operator is generated is given by its RGE. At the one-loop level we have [4,5,6,7]

$$16\pi^2\,\frac{\mathrm{d}\kappa}{\mathrm{d}t} \;=\; C\,(Y_e^\dagger Y_e)^T\,\kappa + C\,\kappa\,(Y_e^\dagger Y_e) + \alpha\,\kappa\,, \tag{3}$$

where $t = \ln(\mu/\mu_0)$ and μ is the renormalization scale[a] and where

$$C = 1 \qquad \text{in the MSSM and } \; C = -\frac{3}{2} \quad \text{in the SM}\,. \tag{4}$$

[a] In the MSSM, the RGE is known at two-loop [8]. In this study, we will, however, focus on the one-loop equation.

In the SM and in the MSSM, α reads

$$\alpha_{\rm SM} = -3g_2^2+2(y_\tau^2+y_\mu^2+y_e^2)+6\big(y_t^2+y_b^2+y_c^2+y_s^2+y_d^2+y_u^2\big)+\lambda, \quad (5a)$$

$$\alpha_{\rm MSSM} = -\frac{6}{5}g_1^2 - 6g_2^2 + 6\left(y_t^2+y_c^2+y_u^2\right) \ . \quad (5b)$$

Here Y_f ($f \in \{e,d,u\}$) represent the Yukawa coupling matrices of the charged leptons, down- and up-quarks, respectively, g_i denote the gauge couplings[b] and λ the Higgs self-coupling. We work in the basis where Y_e is diagonal. The masses are proportional to the eigenvalues of κ and the mixing angles and physical phases are given by the leptonic mixing matrix [9]

$$U = V(\theta_{12},\theta_{13},\theta_{23},\delta)\ {\rm diag}(e^{-{\rm i}\varphi_1/2}, e^{-{\rm i}\varphi_2/2}, 1) \ , \quad (6)$$

which diagonalizes κ in this basis. V is the leptonic analogon to the CKM matrix in the quark sector and we use the standard parameterization [10].

3. Analytical Formulae

In [11] explicit RGEs for the all physical parameters (including CP phases) are given. y_e and y_μ are neglected against y_τ and the expansion parameter

$$\zeta := \frac{\Delta m^2_{\rm sol}}{\Delta m^2_{\rm atm}} \ , \quad (7)$$

is introduced, whose LMA best-fit value is about 0.03. We furthermore define $m_i(t) := v^2\,\kappa_i(t)/4$ with $v = 246\,{\rm GeV}$ in the SM or $v = 246\,{\rm GeV}\cdot\cos\beta$ in the MSSM and, as usual, $\Delta m^2_{\rm sol} := m_2^2 - m_1^2$ and $\Delta m^2_{\rm atm} := m_3^2 - m_2^2$. With these conventions, we obtain for the mixing angles:

$$\dot\theta_{12} = -\frac{Cy_\tau^2}{32\pi^2}\,\sin 2\theta_{12}\,s_{23}^2\,\frac{|m_1\,e^{{\rm i}\varphi_1} + m_2\,e^{{\rm i}\varphi_2}|^2}{\Delta m^2_{\rm sol}} + \mathscr{O}(\theta_{13}) \ , \quad (8)$$

$$\dot\theta_{13} = \frac{Cy_\tau^2}{32\pi^2}\,\sin 2\theta_{12}\,\sin 2\theta_{23}\,\frac{m_3}{\Delta m^2_{\rm atm}\,(1+\zeta)} \times [m_1\cos(\varphi_1-\delta) - (1+\zeta)\,m_2\,\cos(\varphi_2-\delta) - \zeta m_3\,\cos\delta] + \mathscr{O}(\theta_{13}) \ , \quad (9)$$

$$\dot\theta_{23} = -\frac{Cy_\tau^2}{32\pi^2}\,\sin 2\theta_{23}\,\frac{1}{\Delta m^2_{\rm atm}}\left[c_{12}^2\,|m_2\,e^{{\rm i}\varphi_2} + m_3|^2 + s_{12}^2\,\frac{|m_1\,e^{{\rm i}\varphi_1}+m_3|^2}{1+\zeta}\right] + \mathscr{O}(\theta_{13}) \ . \quad (10)$$

[b] We are using GUT charge normalization for g_1.

The $\mathscr{O}(\theta_{13})$ terms in the above RGEs can become important if θ_{13} is not too small and if cancellations appear in the leading terms. This is, for example, the case for $|\varphi_1 - \varphi_2| = \pi$ in (8). The RGE for the Dirac phase is given by

$$\dot{\delta} = \frac{Cy_\tau^2}{32\pi^2}\frac{\delta^{(-1)}}{\theta_{13}} + \frac{Cy_\tau^2}{8\pi^2}\delta^{(0)} + \mathscr{O}(\theta_{13}) \,, \tag{11a}$$

$$\begin{aligned}\delta^{(-1)} = {} & \sin 2\theta_{12}\, \sin 2\theta_{23}\, \frac{m_3}{\Delta m^2_{\rm atm}\,(1+\zeta)} \times [m_1 \sin(\varphi_1 - \delta) \\ & - (1+\zeta)\, m_2\, \sin(\varphi_2 - \delta) + \zeta m_3\, \sin\delta] \,,\end{aligned} \tag{11b}$$

$$\begin{aligned}\delta^{(0)} = {} & \frac{m_1 m_2\, s^2_{23}\, \sin(\varphi_1 - \varphi_2)}{\Delta m^2_{\rm sol}} \\ & + m_3\, s^2_{12} \left[\frac{m_1\, \cos 2\theta_{23}\, \sin\varphi_1}{\Delta m^2_{\rm atm}(1+\zeta)} + \frac{m_2\, c^2_{23}\, \sin(2\delta - \varphi_2)}{\Delta m^2_{\rm atm}}\right] \\ & + m_3\, c^2_{12} \left[\frac{m_1\, c^2_{23}\, \sin(2\delta - \varphi_1)}{\Delta m^2_{\rm atm}(1+\zeta)} + \frac{m_2\, \cos 2\theta_{23}\, \sin\varphi_2}{\Delta m^2_{\rm atm}}\right] .\end{aligned} \tag{11c}$$

The physical Majorana phases are given by

$$\begin{aligned}\dot{\varphi}_1 = {} & \frac{Cy_\tau^2}{4\pi^2}\left\{m_3\, \cos 2\theta_{23}\, \frac{m_1 s^2_{12}\, \sin\varphi_1 + (1+\zeta)\, m_2\, c^2_{12}\, \sin\varphi_2}{\Delta m^2_{\rm atm}\,(1+\zeta)}\right. \\ & \left. + \frac{m_1 m_2\, c^2_{12}\, s^2_{23}\, \sin(\varphi_1 - \varphi_2)}{\Delta m^2_{\rm sol}}\right\} + \mathscr{O}(\theta_{13}) \,,\end{aligned} \tag{12}$$

$$\begin{aligned}\dot{\varphi}_2 = {} & \frac{Cy_\tau^2}{4\pi^2}\left\{m_3\, \cos 2\theta_{23}\, \frac{m_1 s^2_{12}\, \sin\varphi_1 + (1+\zeta)\, m_2\, c^2_{12} \sin\varphi_2}{\Delta m^2_{\rm atm}\,(1+\zeta)}\right. \\ & \left. + \frac{m_1 m_2\, s^2_{12}\, s^2_{23}\, \sin(\varphi_1 - \varphi_2)}{\Delta m^2_{\rm sol}}\right\} + \mathscr{O}(\theta_{13}) \,.\end{aligned} \tag{13}$$

The above expressions can be further simplified by neglecting ζ against 1. Note that singularities can appear in the $\mathscr{O}(\theta_{13})$-terms at points in parameter space, where the phases are not well-defined. For the masses, the results for $y_e = y_\mu = 0$ but arbitrary θ_{13} are

$$16\pi^2\, \dot{m}_1 = \left[\alpha + Cy_\tau^2\, \left(2 s^2_{12}\, s^2_{23} + F_1\right)\right] m_1 \,, \tag{14a}$$

$$16\pi^2\, \dot{m}_2 = \left[\alpha + Cy_\tau^2\, \left(2 c^2_{12}\, s^2_{23} + F_2\right)\right] m_2 \,, \tag{14b}$$

$$16\pi^2\, \dot{m}_3 = \left[\alpha + 2Cy_\tau^2\, c^2_{13}\, c^2_{23}\right] m_3 \,, \tag{14c}$$

where F_1 and F_2 contain terms proportional to $\sin\theta_{13}$,

$$F_1 = -s_{13}\, \sin 2\theta_{12}\, \sin 2\theta_{23}\, \cos\delta + 2 s^2_{13}\, c^2_{12}\, c^2_{23} \,, \tag{15a}$$

$$F_2 = s_{13}\, \sin 2\theta_{12}\, \sin 2\theta_{23}\, \cos\delta + 2 s^2_{13}\, s^2_{12}\, c^2_{23} \,. \tag{15b}$$

These formulae lead to RGEs for the mass squared differences,

$$8\pi^2 \frac{\mathrm{d}}{\mathrm{d}t}\Delta m^2_{\rm sol} = \alpha\, \Delta m^2_{\rm sol} + C y_\tau^2 \left[2 s^2_{23} \left(m_2^2\, c^2_{12} - m_1^2\, s^2_{12}\right) + F_{\rm sol}\right] , \quad (16a)$$

$$8\pi^2 \frac{\mathrm{d}}{\mathrm{d}t}\Delta m^2_{\rm atm} = \alpha\, \Delta m^2_{\rm atm} + C y_\tau^2 \left[2 m_3^2\, c^2_{13}\, c^2_{23} - 2 m_2^2\, c^2_{12}\, s^2_{23} + F_{\rm atm}\right] \quad (16b)$$

where

$$F_{\rm sol} = \left(m_1^2 + m_2^2\right) s_{13}\, \sin 2\theta_{12}\, \sin 2\theta_{23}\, \cos\delta + 2 s^2_{13}\, c^2_{23} \left(m_2^2\, s^2_{12} - m_1^2\, c^2_{12}\right) , \quad (17a)$$

$$F_{\rm atm} = -m_2^2\, s_{13}\, \sin 2\theta_{12}\, \sin 2\theta_{23}\, \cos\delta - 2 m_2^2\, s^2_{13}\, s^2_{12}\, c^2_{23} . \quad (17b)$$

4. RG Evolution of θ_{13}, θ_{23}, θ_{12}

An interesting question is if deviations from $\theta_{13} = 0$ and $\theta_{23} = \pi/4$ at low energies could be the consequence of radiative corrections. Therefore we study RG corrections to θ_{13} and θ_{23} from the running of the effective neutrino mass operator between the see-saw scale and the electroweak scale[c].

The corrections to θ_{13} are in a good approximation described by the leading term which does not depend on θ_{13}. Then $\dot\theta_{13} \simeq$ const. in Eq. (9), i.e. a constant slope depending on the Dirac CP phase δ and the Majorana phases φ_1 and φ_2. Assuming at some high scale M_1 where neutrino masses are generated $\theta_{13} = 0$, Eq. (9) allows to determine the RG corrections at $10^2\,\mathrm{GeV}$. For the examples we take $M_1 = 10^{12}\,\mathrm{GeV}$ and the approximate size of the RG corrections to $\sin^2 2\theta_{13}$ in the MSSM is shown in Fig. 2. In the upper diagram it is plotted as a function of $\tan\beta$ and the lightest neutrino mass m_1 for constant Majorana phases $\varphi_1 = 0$ and $\varphi_2 = \pi$. The lower diagram shows the dependence of the corrections on φ_1 and φ_2 for $\tan\beta = 50$ and $m_1 = 0.08\,\mathrm{eV}$ in the case of a normal mass hierarchy. The diagrams look rather similar for an inverted hierarchy. Analytically, the pattern of the upper plot is easy to understand, and for the lower one there is a simple explanation as well. Consider partially or nearly degenerate neutrino masses. Then Eq. (9) yields to a reasonably good approximation

$$\dot\theta_{13} \approx \frac{C y_\tau^2}{32\pi^2}\, \sin 2\theta_{12}\, \sin 2\theta_{23}\, \frac{m^2}{\Delta m^2_{\rm atm}} \left[\cos(\varphi_1 - \delta) - \cos(\varphi_2 - \delta)\right] \propto \sin\frac{\varphi_1 + \varphi_2 - 2\delta}{2}\, \sin\frac{\varphi_1 - \varphi_2}{2} . \quad (18)$$

[c]The potential of future long-baseline neutrino oscillation experiments to determine deviations from maximal $\nu_\mu - \nu_\tau$ mixing was discusses in [12].

This gives an understanding of the diagonal bands in Fig. 2, in particular the white one corresponding to $\varphi_1 - \varphi_2 = 0$.

Planned reactor experiments [13] and next generation superbeam experiments [14,15] are expected to have an approximate sensitivity on $\sin^2 2\theta_{13}$ of 10^{-2}. From Fig. 2 we find that the radiative corrections exceed this value for large regions of the currently allowed parameter space, unless there are cancellations due to Majorana phases, i.e. $\varphi_1 = \varphi_2$. If so, the effects are generically smaller than 10^{-2} as can be seen from the lower diagram. Future upgraded superbeam experiments like JHF-HyperKamiokande have the potential to further push the sensitivity to about 10^{-3} and with a neutrino factory even about 10^{-4} might be reached.

From the theoretical point of view, one would expect that even if some model predicted $\theta_{13} = 0$ at the energy scale of neutrino mass generation, RG effects would at least produce a non-zero value of the order shown in Fig. 2. Consequently, experiments with such a sensitivity have a large discovery potential for θ_{13}. We should point out that this is a conservative estimate, since if neutrino masses are e.g. determined by GUT scale physics, model-dependent radiative corrections in the region between M_1 and $M_{\rm GUT}$ contribute as well [16,17,18,19] and there can be additional corrections from physics above the GUT scale [20]. On the other hand, if experiments do not measure θ_{13}, this will improve the upper bound on θ_{13}. Parameter space regions where the corrections are larger than this bound will then appear unnatural from the theoretical side.

Next we consider the RG corrections to θ_{23}, where very interesting questions arise if θ_{23} turns out to be close to $\pi/4$. The deviation of θ_{23} from $\pi/4$ might again be an effect of the RG running which induces a deviation of θ_{23} from $\pi/4$. In order to understand the corrections we use the analytical formula (10) with a constant right-hand side in order to calculate the running in the MSSM between M_Z and the see-saw scale, where we take again $M_1 = 10^{12}\,\text{GeV}$ for our examples. As initial conditions we assume small θ_{13} at M_1 and low-energy best-fit values for the remaining lepton mixings and the neutrino mass squared differences. In leading order in θ_{13}, the evolution is of course independent of the Dirac phase δ.

The size of the RG corrections in the MSSM is shown in Fig. 3. From the upper diagram it can be read off for desired values of $\tan\beta$ and the lightest mass eigenvalue m_1 in an example with vanishing Majorana phases. The lower diagram shows its dependence on the Majorana phases φ_1 and φ_2 for $\tan\beta = 50$, $m_1 = 0.1\,\text{eV}$ and a normal mass hierarchy. The diagrams look rather similar in the case of an inverted hierarchy. The effects of the

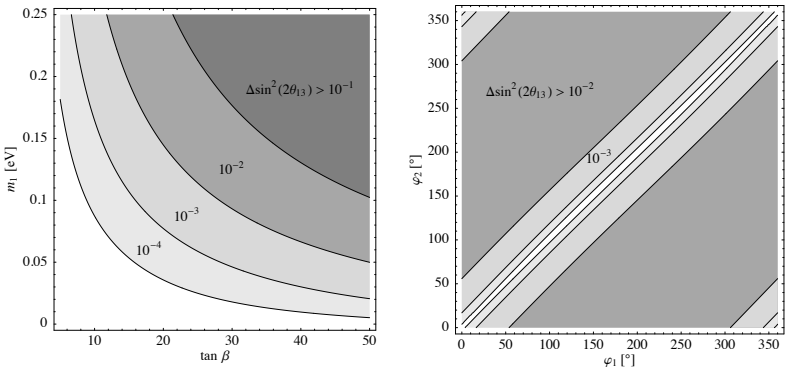

Figure 2. Corrections to θ_{13} from the RG evolution between 10^2 and 10^{12} GeV in the MSSM, calculated using the analytical approximations with initial conditions $\theta_{13} = 0$ and LMA best-fit values for the remaining parameters. The upper diagram shows the dependence on $\tan\beta$ and on the mass of the lightest neutrino for the case of a normal mass hierarchy and phases $\varphi_1 = 0$ and $\varphi_2 = \pi$. In the lower diagram the dependence on the Majorana phases φ_1 and φ_2 is shown for $\tan\beta = 50$ and $m_1 = 0.08\,\text{eV}$. The contour lines are defined as in the upper diagram.

Majorana phases can easily be understood from Eq. (10). In the region with $\varphi_1 \approx \varphi_2 \approx \pi$, both $|m_2\, e^{\mathrm{i}\varphi_2} + m_3|^2$ and $|m_1\, e^{\mathrm{i}\varphi_1} + m_3|^2$ are small for quasi-degenerate neutrinos, which gives the ellipse with small radiative corrections in the center of the lower diagram. Such cancellations are not possible with hierarchical masses, but the RG effects are generally not very large in this case, as shown by the upper plot.

Even if a model predicted $\theta_{23} = \pi/4$ at some high energy scale, we would thus expect radiative corrections to produce at least a deviation from this value of the size shown in Fig. 3, so that experiments with such a sensitivity are expected to measure a deviation of θ_{23} from $\pi/4$. The sensitivity to $\sin^2 2\theta_{23}$ of future superbeam experiments like T2K is expected to be approximately 1% (see e.g. [21]). This can now be compared with Fig. 3. We find that the radiative corrections exceed this value for large regions of the currently allowed parameter space, where no significant cancellations due to Majorana phases occur. This means that φ_1 and φ_2 must not be to close to π. Otherwise, the effects are generically smaller as can be seen from the lower diagram. Upgraded superbeam experiments or a neutrino factory might even reach a sensitivity of about 0.5%. As argued for the case of θ_{13}, if experiments measure θ_{23} rather close to $\pi/4$, parameter combinations implying larger radiative corrections than the measured deviation will appear unnatural from the theoretical point of view.

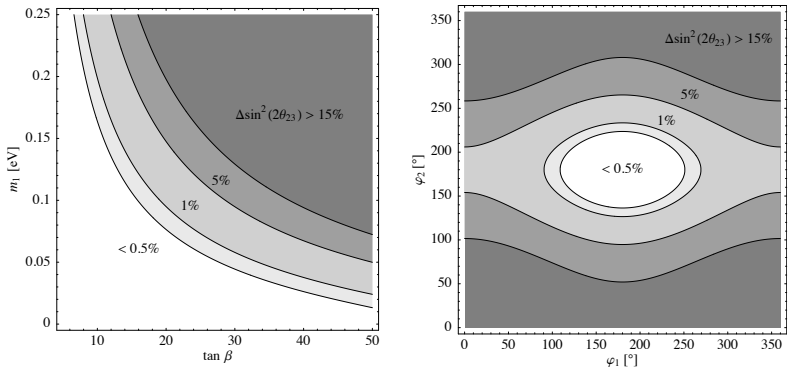

Figure 3. Corrections to θ_{23} from the RG evolution between 10^2 GeV and 10^{12} GeV in the MSSM, calculated from the analytical approximation Eq. (10) with initial conditions $\theta_{23} = \pi/4$, small $\theta_{13} = 0$ and LMA best-fit values for the remaining parameters. The upper diagram shows the dependence on $\tan\beta$ and on the mass m_1 of the lightest neutrino for the case of a normal mass hierarchy and phases $\varphi_1 = \varphi_2 = 0$. In the lower diagram the dependence on the Majorana phases φ_1 and φ_1 is shown for the example $\tan\beta = 50$ and $m_1 = 0.1$. Note that for small θ_{13} the results are independent of the Dirac phase to a good approximation.

Next we discuss the RG Evolution of θ_{12}. From Eq. 8 we see that the running of the solar angle θ_{12} is proportional to $(\Delta m^2_{sol})^{-1}$, while the running of the other angles is proportional to $(\Delta m^2_{atm})^{-1}$. Therefore, $\Delta m^2_{sol}) \ll \Delta m^2_{atm})$ explains why θ_{12} has generically the strongest RG effects among the mixing angles, especially for for quasi-degenerate neutrinos and for the case of an inverted mass hierarchy. Furthermore, it is known that in the MSSM the solar angle always increases when running down from M_1 for $\theta_{13} = 0$ [22]. This is confirmed by our formula (8). From the term $|m_1\, e^{\mathrm{i}\varphi_1} + m_2\, e^{\mathrm{i}\varphi_2}|^2$ in Eq. (8), we see that a non-zero value of the difference $|\varphi_1 - \varphi_2|$ of the Majorana phases damps the RG evolution. The damping becomes maximal if this difference equals π, which corresponds to an opposite CP parity of the mass eigenstates m_1 and m_2. This is in agreement with earlier studies, e.g. [23,24,25].

Let us now compare the analytical approximation for $\dot{\theta}_{12}$ of Eq. (8) with the numerical solution for the running in the case of nearly degenerate masses, which is shown in Fig. 4. The dark-gray region shows the evolution with LMA best-fit values for the neutrino parameters, θ_{13} varying in the interval $[0°, 9°]$ and all CP phases equal to zero. The medium-gray regions show the evolution for $|\varphi_1 - \varphi_2| \in \{\, 0°, 90°, 180°, 270°\}$, $\theta_{13} \in [0°, 9°]$ and $\delta \in \{0°, 90°, 180°, 270°\}$, confirming the expectation of the damping influence

of φ_1 and φ_2. The flat line at low energy stems from the SM running below $M_{\rm SUSY}$, which is negligible.

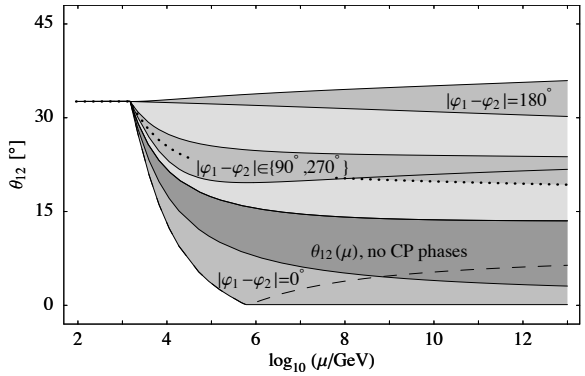

Figure 4. RG evolution of θ_{12} in the MSSM with $\tan\beta = 50$, a normal mass hierarchy and $m_1 = 0.1\,\text{eV}$. The dark-gray region shows the evolution with best-fit values for the neutrino parameters, $\theta_{13} \in [0°, 9°]$ and all CP phases equal to zero. The medium-gray regions show the evolution for $|\varphi_1 - \varphi_2| = 0°$, $|\varphi_1 - \varphi_2| \in \{90°, 270°\}$ and $|\varphi_1 - \varphi_2| = 180°$. They emerge from varying $\theta_{13} \in [0°, 9°]$ and $\delta \in \{0°, 90°, 180°, 270°\}$. The light-gray regions can be reached by choosing specific values for the CP phases different from the ones listed above. The dashed line shows the RG evolution with $|\varphi_1 - \varphi_2| = 0$, $\theta_{13} = 9°$ and $\delta = 180°$. Note that for the numerics we use the convention where θ_{12} is restricted to the interval $[0°, 45°]$, so that the angle increases again after reaching 0. The dotted line shows the evolution with $|\varphi_1 - \varphi_2| = 90°$ and $\theta_{13} = 0°$.

In the case of large cancellations by phases, the $\mathscr{O}(\theta_{13})$-term in the RGE turns out to be important. The dominant contribution to the next-to-leading term is given by Υ where

$$\Upsilon = \frac{C y_\tau^2}{32\pi^2} \frac{m_2 + m_1}{m_2 - m_1} \cos\left(\frac{\varphi_1 - \varphi_2}{2}\right) \times \\ \times \left[\cos(2\theta_{12})\,\cos\delta\,\cos\left(\frac{\varphi_1 - \varphi_2}{2}\right) + \sin\delta\,\sin\left(\frac{\varphi_1 - \varphi_2}{2}\right)\right] \cdot \theta_{13}\,. \quad (19)$$

Clearly, the RG evolution of θ_{12} is independent of the Dirac phase δ only in the approximation $\theta_{13} = 0$. The largest running, where θ_{12} can even become zero, occurs for θ_{13} as large as possible (9°), $\delta = \pi$ and $\varphi_1 - \varphi_2 = 0$. In this case the leading and the next-to-leading term add up constructively. It is also interesting to observe that due to $\mathscr{O}(\theta_{13})$ effects θ_{12} can run to slightly larger values. The damping due to the Majorana phases is maximal in this case, which almost eliminates the leading term. Then, all the running comes from the next-to-leading term (19).

In the inverted scheme, $m_1 \gg m_2 - m_1$ always holds, so that large RG effects are generic, i.e. always present except for the case of cancellations due to Majorana phases. For a normal mass hierarchy with a small m_1, the running of the solar mixing is of course rather insignificant.

Finally, we would like to emphasize that it is not appropriate to assume the right-hand sides of Eq. (8) and Eq. (19) to be constant in order to interpolate θ_{12} up to a high energy scale, since non-linear effects especially from the running of $\sin 2\theta_{12}$ and $\Delta m^2_{\rm sol}$ cannot be neglected here. This is easily seen from the curved lines in Fig. 4.

5. RG Corrections to Leptogenesis Parameters

One of the most attractive mechanisms for explaining the observed baryon asymmetry of the universe, $\eta_B = (6.5^{+0.4}_{-0.8}) \cdot 10^{-10}$ [26], is leptogenesis [27]. In this scenario, η_B is generated by the out-of-equilibrium decay of the same heavy singlet neutrinos which are responsible for the suppression of light neutrino masses in the see-saw mechanism. The masses of the heavy neutrinos are typically assumed to be some orders of magnitude below the GUT scale. Though the parameters entering the leptogenesis mechanism cannot be completely expressed in terms of low-energy neutrino mass parameters, it is possible to derive bounds on the neutrino mass scale from requiring successful leptogenesis [28]. However, since leptogenesis occurs at high temperatures and correspondingly at high scales, one cannot directly use the low energy parameters and the RGE evolution has to be taken into account. The neutrino masses experience corrections of about 20-25% in the MSSM or more than 60% in the SM and we expect therefore sizable corrections to the leptogenesis bounds. The maximal baryon asymmetry generated in the thermal version of this scenario is given by [29,30,28]

$$\eta_B^{\rm max} \simeq 0.96 \cdot 10^{-2}\, \varepsilon_1^{\rm max}\, \kappa_{\rm f} \,. \tag{20}$$

$\kappa_{\rm f}$ is a dilution factor which can be computed from a set of coupled Boltzmann equations (see, e.g. [31]). In [28], an analytic expression for the maximal relevant CP asymmetry was derived,

$$\varepsilon_1^{\rm max}(m_1, m_3, \widetilde{m}_1) = \frac{3}{16\pi} \frac{M_1\, m_3}{(v/\sqrt{2})^2} \left[1 - \frac{m_1}{m_3}\left(1 + \frac{m_3^2 - m_1^2}{\widetilde{m}_1^2}\right)^{1/2}\right] \tag{21}$$

which refines the older bound

$$\varepsilon_1^{\rm max}(m_1, m_3) = \frac{3}{16\pi} \frac{M_1}{(v/\sqrt{2})^2} \frac{\Delta m^2_{\rm atm} + \Delta m^2_{\rm sol}}{m_3} \tag{22}$$

and is valid for a normal mass hierarchy in the SM as well as in the MSSM.[d] $\widetilde{m}_1$ is defined by

$$\widetilde{m}_1 = \frac{(m_{\rm D}^\dagger m_{\rm D})_{11}}{M_1} \tag{23}$$

with $m_{\rm D} \sim Y_\nu$ being the neutrino Dirac mass and typically lies between m_1 and m_3. It can be constrained by the requirement of successful leptogenesis because it controls the dilution of the generated asymmetry. The authors of [28] introduced the 'neutrino mass window for baryogenesis' which corresponds to the region in the $\widetilde{m}_1$-M_1 plane allowing for successful thermal leptogenesis. The shape and size of the 'mass window' depends on $\overline{m} = \sqrt{m_1^2 + m_2^2 + m_3^2}$, i.e. it becomes smaller for increasing $\overline{m}$, and $\overline{m} \geq 0.2\,\text{eV}$ is not compatible with thermal leptogenesis.

The calculations relevant for leptogenesis, however, refer to processes at very high energies, and therefore the RG evolution of the input parameters has to be taken into account [32]. The size of the error arising if RG effects are neglected has been estimated in [11]. It was found that there are two effects in opposite directions: The CP asymmetry is enhanced because the mass squared differences increase, and the dilution of the baryon asymmetry is more effective since the overall mass scale rises due to RG effects. As the dependence of the dilution factor on the mass scale is stronger than that of the CP asymmetry, it is expected that the mass window for baryogenesis shrinks when RG effects are included in the analysis. An exception is the case of large $\tan\beta$, where the situation is more complicated.

There exist also different other, non-thermal baryogenesis mechanisms [35] in which the masses of the light neutrinos may be almost degenerate [36]. In these kinds of scenarios, RG effects increase the baryon asymmetry, since ε_1 increases, while the effects from the expected decrease of the dilution factor do not occur.

6. Conclusions

We discussed the RG running of neutrino parameters. Analytical solutions of the running mixings and masses were presented and phenomenologiacl consequences were discussed for leptogenesis. Further phenomenological issues and possibilities as, for example, the radiative generation of CP Phases,

[d] To use these formulae in our conventions for the inverted scheme, one would have to replace $(m_1, m_2, m_3) \to (m_3, m_1, m_2)$.

are discussed in [11]. Running above the see-saw threshold leads also to important effects and this will be discussed in a forthcoming paper.

References

1. B. Grzadkowski, M. Lindner, Phys. Lett. **B193** (1987) 71.
2. B. Grzadkowski, M. Lindner, S. Theisen, Phys. Lett. **B198** (1987) 64.
3. E. Ma, Phys. Rev. Lett. **81** (1998), 1171.
4. P. H. Chankowski, Z. Pluciennik, Phys. Lett. **B316** (1993), 312.
5. K. S. Babu, C. N. Leung, J. Pantaleone, Phys. Lett. **B319** (1993), 191.
6. S. Antusch, M. Drees, J. Kersten, M. Lindner, M. Ratz, Phys. Lett. **B519** (2001), 238.
7. S. Antusch, M. Drees, J. Kersten, M. Lindner, M. Ratz, Phys. Lett. **B525** (2002), 130.
8. S. Antusch, M. Ratz, JHEP **07** (2002), 059.
9. Z. Maki, M. Nakagawa, S. Sakata, Prog. Theor. Phys. **28** (1962), 870.
10. standard parametrization
11. S. Antusch, J. Kersten, M. Lindner, M. Ratz, Nucl. Phys. **B674** (2003) 401.
12. S. Antusch, P. Huber, J. Kersten, T. Schwetz, W. Winter, `hep-ph/0404268`.
13. P. Huber, M. Lindner, T. Schwetz, W. Winter, Nucl.Phys. **B665** (2003) 487.
14. P. Huber, M. Lindner, W. Winter, Nucl. Phys. **B654** (2003), 3.
15. H. Minakata, H. Nunokawa, S. Parke, Phys.Rev. **D68** (2003) 013010.
16. S. F. King, N. N. Singh, Nucl. Phys. **B591** (2000), 3.
17. S. Antusch, J. Kersten, M. Lindner, M. Ratz, Phys. Lett. **B538** (2002) 87.
18. S. Antusch, J. Kersten, M. Lindner, M. Ratz, Phys. Lett. **B544** (2002) 1.
19. S. Antusch, M. Ratz, JHEP **11** (2002), 010.
20. F. Vissani, M. Narayan, V. Berezinsky, Phys.Lett. **B571** (2003) 209.
21. Y. Itow et al., *The JHF-Kamioka neutrino project*, (2001), `hep-ex/0106019`.
22. T. Miura, T. Shindou, E. Takasugi, Phys. Rev. **D66** (2002), 093002.
23. K. R. S. Balaji, A. S. Dighe, R. N. Mohapatra, M. K. Parida, Phys. Rev. Lett. **84** (2000), 5034.
24. N. Haba, Y. Matsui, N. Okamura, Eur. Phys. J. **C17** (2000), 513.
25. P. H. Chankowski, S. Pokorski, Int. J. Mod. Phys. **A17** (2002), 575.
26. D. N. Spergel et al., (2003), `astro-ph/0302209`.
27. M. Fukugita, T. Yanagida, Phys. Lett. **174B** (1986), 45.
28. W. Buchmüller, P. D. Bari, M. Plümacher, (2003), `hep-ph/0302092`.
29. K. Hamaguchi, H. Murayama, T. Yanagida, Phys. Rev. **D65** (2002), 043512.
30. S. Davidson, A. Ibarra, Phys. Lett. **B535** (2002), 25.
31. W. Buchmüller, M. Plümacher, Int. J. Mod. Phys. **A15** (2000), 5047.
32. R.Barbieri, P.Creminelli, A.Strumia, N.Tetradis, Nucl.Phys. **B575** (2000),61.
33. H. B. Nielsen, Y. Takanishi, Nucl. Phys. **B636** (2002), 305.
34. P. Di Bari, AIP Conf.Proc. **655** (2003) 208.
35. K. Kumekawa, T. Moroi, T. Yanagida, Prog. Theor. Phys. **92** (1994), 437.
36. M. Fujii, K. Hamaguchi, T. Yanagida, Phys. Rev. **D65** (2002), 115012.